

## Electronic Supplementary Information

to

# **NMR-Crystallographic Study of Two-Dimensionally Self-Assembled Cyclohexane Based Low-Molecular-Mass Organic Compounds†**

Marko Schmidt,<sup>a</sup> Christoph S. Zehe,<sup>a</sup> Renée Siegel,<sup>a</sup> Johannes U. Heigl,<sup>b</sup>  
Christoph Steinlein,<sup>b</sup> Hans-Werner Schmidt<sup>b</sup> and Jürgen Senker<sup>\*a</sup>

<sup>a</sup> Inorganic Chemistry III and Bayreuth Center for Colloids and Interfaces, University of Bayreuth, Universitätsstr. 30, 95447 Bayreuth, Germany.

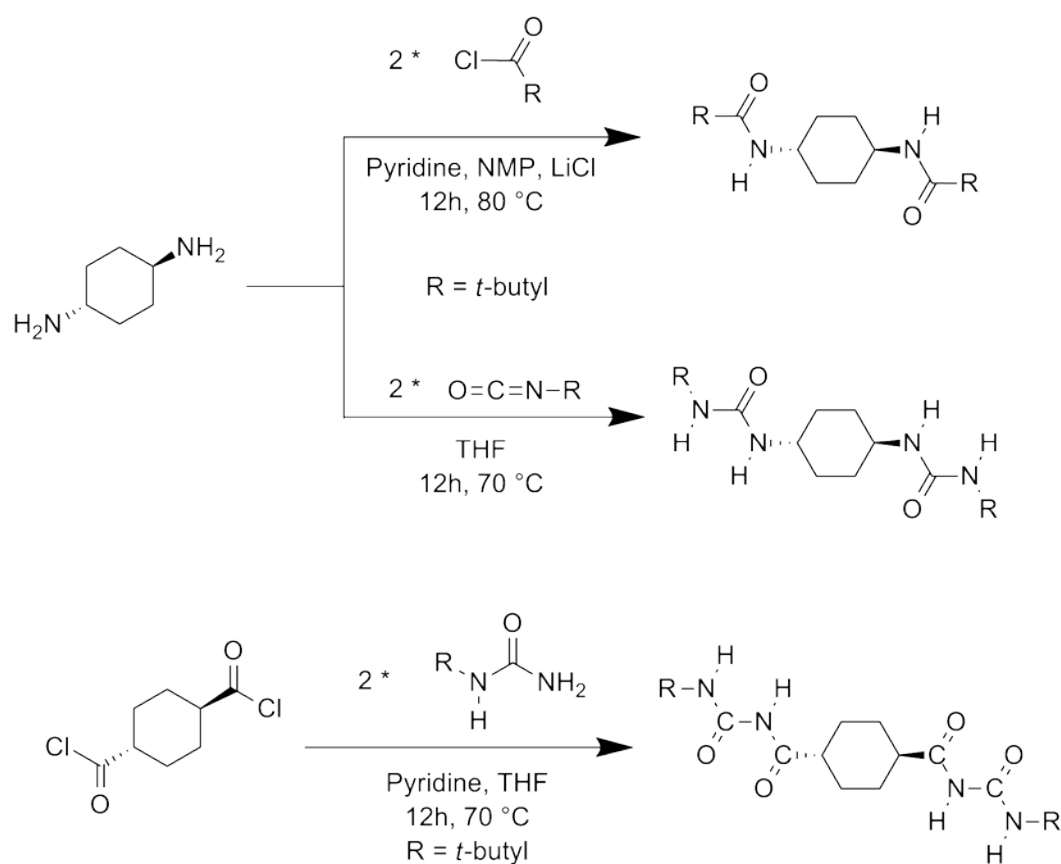
Tel: +49(0)921552532; E-mail: [juergen.senker@uni-bayreuth.de](mailto:juergen.senker@uni-bayreuth.de)

<sup>b</sup> Macromolecular Chemistry I, Bayreuth Institute of Macromolecular Research and Bayreuth Center for Colloids and Interfaces, University of Bayreuth, Universitätsstr. 30, 95447 Bayreuth, Germany.

Tel: +49(0)921553200; E-mail: [hans-werner.schmidt@uni-bayreuth.de](mailto:hans-werner.schmidt@uni-bayreuth.de)

### Synthesis of compounds 1 - 3

The principal reaction schemes of the classical addition and elimination reactions is visualised in Scheme S1. The full conversion of the educts as well as the purity of the products was confirmed by means of elementary analysis (CHN), mass spectrometry and powder X-ray diffraction. The CHN analysis revealed a good agreement between calculated and experimental values (compare experimental section in the main article).



**Scheme S1** Schematic representation of the synthetic routes to obtain **1** and **2** (based on *trans*-1,4-diaminocyclohexane) and **3** (based on cyclohexane-*trans*-1,4-dicarbonyl dichloride).

### Explanation of the $^{14}\text{N}$ - effect

A comparison of  $^{13}\text{C}$  CP measurements on 300 MHz and 400 MHz spectrometers is depicted in Figure S1a. Here, for each compound the spectrum measured at higher field shows a decrease of the splitting. This is in accordance with the trend of the second-order quadrupolar interaction which depends inversely on the field strength. For  $^1\text{H}$ , the influence of  $^{14}\text{N}$  can be visualised in the same way by comparing one-pulse proton spectra measured at different magnetic fields. Exemplarily, this is pointed out for compound **1** in Figure S1b. Here, the blue line represents a  $^1\text{H}$  one-pulse experiment at a proton frequency of 400 MHz with  $\nu_{\text{rot}} = 22.5$  kHz (bottom), while the backline corresponds to a measurement at a 300 MHz device with  $\nu_{\text{rot}} = 32.5$  kHz (top). The former shows only one signal without additional splitting perfectly matching with the molecular structure obtained for **1**. The latter one, on the other hand, possesses a shoulder which can easily be misinterpreted as a second signal but is based on the  $^{14}\text{N}$  interaction. Complementary results are obtained for **2** and **3** (not shown here).

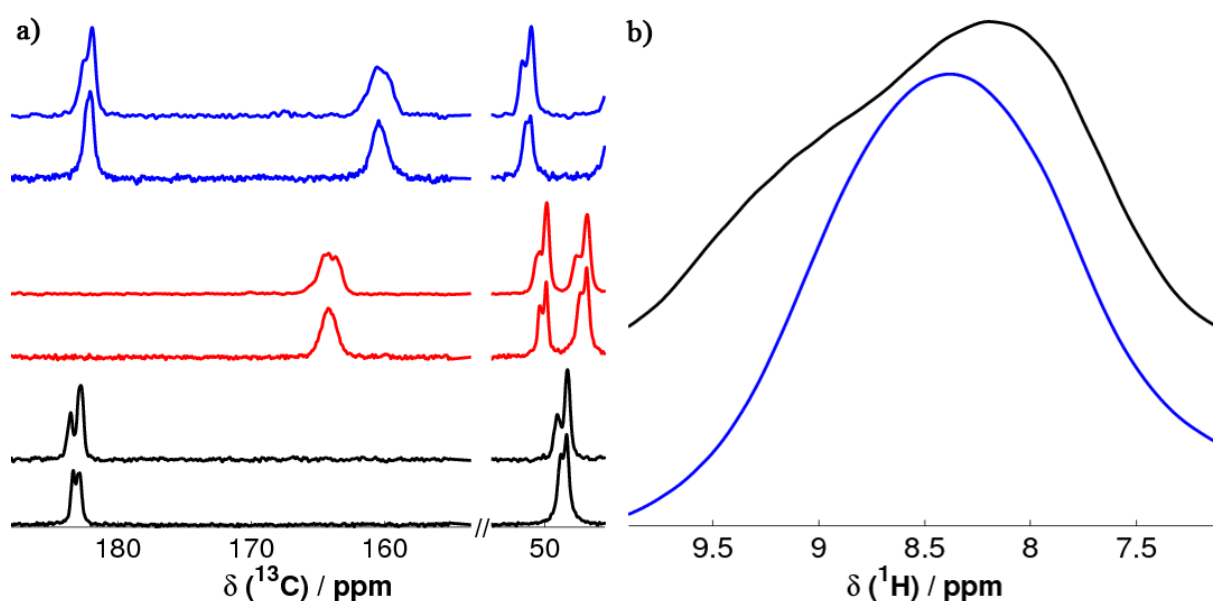


**Fig. S1** (a)  $^{13}\text{C}$  CP spectra of the three compounds (black = **1**, red = **2**, blue = **3**), where for each compound the lower spectrum corresponds to proton frequency of 400 MHz and the upper spectrum to 300 MHz; all spectra are recorded at a spinning rate of 10 kHz; (b)  $^1\text{H}$  one-pulse spectra of compound **3** measured at a proton frequency of 400 MHz and a rotation frequency of 22.5 kHz (blue line, bottom) and 300 MHz at a rotation frequency of 32.5 kHz (black line, top).

To strengthen this argument, simulations of both  $^{13}\text{C}$  CP and  $^1\text{H}$  DUMBO spectra (both measured at  $B_0 = 7.04$  T) including a  $^{14}\text{N}$  effect were performed using the freeware program WSOLIDS1.<sup>1</sup> The simulations were done exemplarily for  $\text{C}_6$  and  $\text{H}_3$  (compare Table 2 in the main article) within the acylurea unit of compound **3** since the resonances of these nuclei are sustainably influenced by the neighbored  $^{14}\text{N}$  nucleus. For getting reasonable starting values for  $^{13}\text{C}$ , a comparable OC-NH system was taken from literature.<sup>2</sup> Here the quadrupolar coupling constant ( $C_Q = -3.2$  MHz), the asymmetry parameter ( $\eta = 0.22$ ), the azimuth angle of the internuclear  $^{13}\text{C}$ - $^{14}\text{N}$  vector in the principal axis system of the electric field gradient (EFG) tensor ( $\alpha = 43^\circ$ ) as well as the polar angle of the internuclear  $^{13}\text{C}$ - $^{14}\text{N}$  vector in the principal axis system of the EFG tensor ( $\beta = 90^\circ$ ) were extracted. The isotropic chemical shift was set to  $\delta = 177.15$  ppm while the direct dipolar coupling constant ( $d_{\text{C}-^{14}\text{N}}^{13} = 840$  Hz) was calculated according to the crystal structure obtained by PXRD. For the indirect scalar dipolar coupling between  $^{13}\text{C}$  and  $^{14}\text{N}$  (“ $J$ -coupling”) 7 Hz was adjusted. A similar procedure was performed for the  $^1\text{H}$  spectrum. Due to the same orientations of the EFG tensors of both  $^{14}\text{N}$  nuclei the values for  $C_Q$  and  $\eta$  are equal. The isotropic chemical shift was set to  $\delta = 8.29$  ppm while the direct dipolar coupling constant ( $d_{\text{H}-^{14}\text{N}}^1 = 8250$  Hz) was calculated according to the crystal structure. For the indirect scalar dipolar coupling between  $^1\text{H}$  and  $^{14}\text{N}$  65 Hz was chosen which was recalculated from  $^1J(^1\text{H},^{15}\text{N})$ -couplings of comparable compounds from literature.<sup>3</sup> For both simulations, the values of the direct as well as scalar dipolar coupling constant were not varied while all other values were refined during the simulation. Both the simulated and experimental spectra are depicted in Figure S2. For a more detailed description of the theoretical background the reader is referred to ref. 2.

**Table S1** Summary of the parameters used for the simulations of the  $^1\text{H}$  and  $^{13}\text{C}$  spectrum, respectively.

	$^1\text{H}$ ( $\text{H}_3$ )	$^{13}\text{C}$ ( $\text{C}_6$ )
$\delta_{\text{CS}} / \text{ppm}$	8.29	177.15
$d_{\text{X}-^{14}\text{N}} / \text{Hz}$	8250	840
$J_{\text{X}-^{14}\text{N}} / \text{Hz}$	65	7
$C_Q / \text{MHz}$	-3.1	-3.1
$\eta$	0.42	0.4
$\alpha / ^\circ$	5	44
$\beta / ^\circ$	85	85

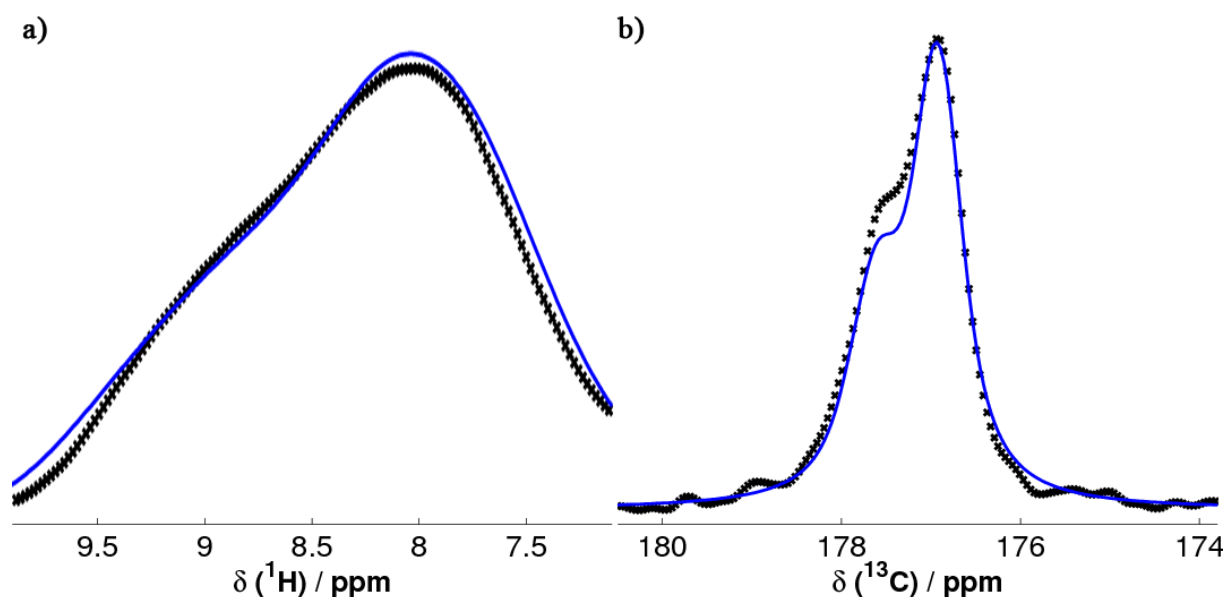


**Fig S2** Experimental spectra from Figure S1 (black crosses) and simulated spectra of H<sub>3</sub> (a) and C<sub>6</sub> (b) (blue lines, compare Table S1) of the acylurea unit of compound **3**.

### Prediction of <sup>13</sup>C and <sup>15</sup>N chemical shifts

**Table S2** Predicted solution-state NMR chemical shifts<sup>4</sup> for the carbon atoms of the carbonyl groups as well as the nitrogen atoms of compounds **1** - **3**. Since the <sup>15</sup>N calculations are performed without proton decoupling only a mean value is shown, without taking into account any <sup>1</sup>J(<sup>1</sup>H,<sup>15</sup>N)-couplings. All values are based on single molecule calculations without considering any inter- or intramolecular interaction, e.g. hydrogen bonding.

	<b>1</b>	<b>2</b>	<b>3</b>	Unit
C <sub>4</sub>	178.5	158.1	155.7	C=O
C <sub>6</sub>	-	-	179.4	C=O
N <sub>3</sub>	-	-278.2	-277.2	NH
N <sub>5</sub>	-250.9	-274.8	-246.0	NH

### HETCOR spectra of compound 1 and 2

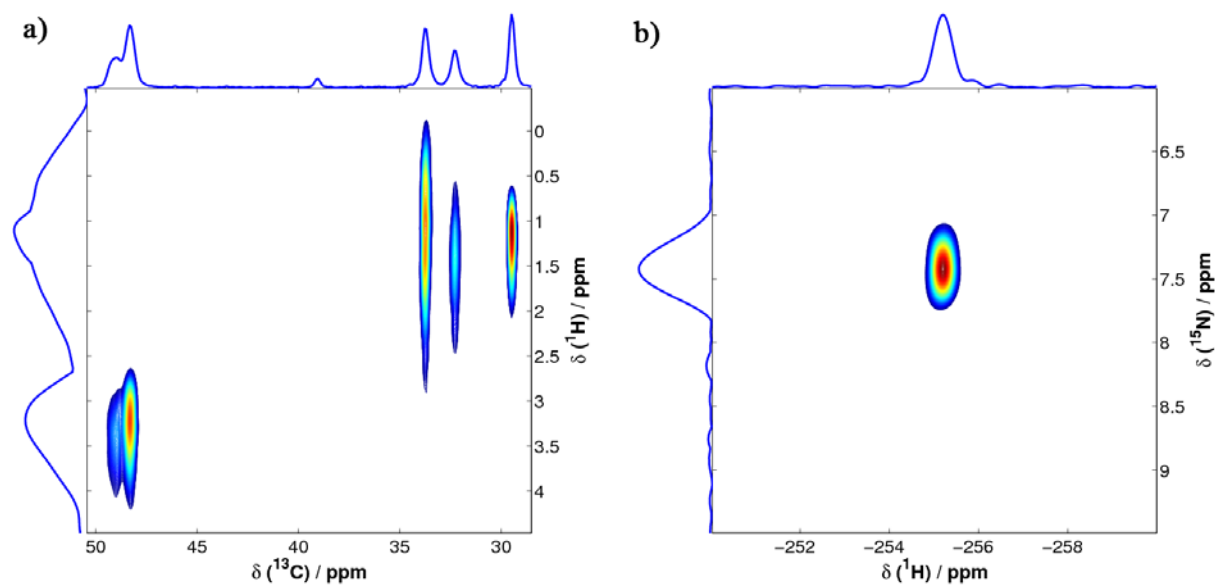


**Fig S3**  $^1\text{H}$ - $^{13}\text{C}$ -HETCOR on a 300 MHz spectrometer (left) and  $^1\text{H}$ - $^{15}\text{N}$ -HETCOR on a 400 MHz spectrometer (right) of compound **1** at a spinning speed of 10 kHz each. The contact time was set to 178  $\mu\text{s}$ .

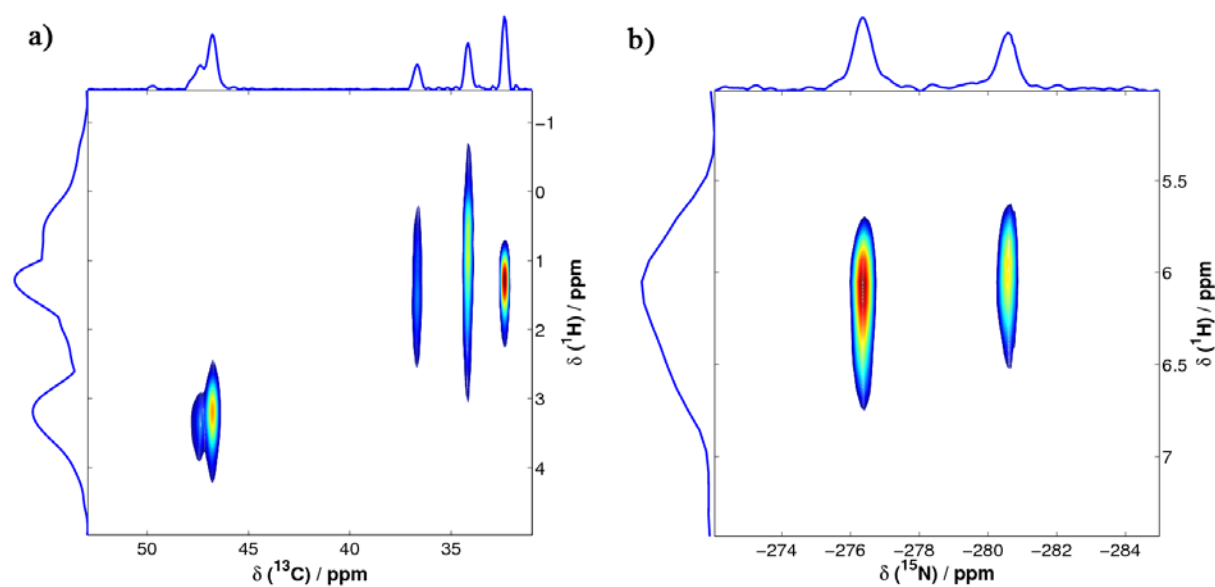


**Fig S4**  $^1\text{H}$ - $^{13}\text{C}$ -HETCOR (left) and  $^1\text{H}$ - $^{15}\text{N}$ -HETCOR (right) spectrum of compound **2** at a spinning speed of 10 kHz on a 300 MHz spectrometer. The contact time was set to 178  $\mu\text{s}$ .

### $^1\text{H}$ - $^1\text{H}$ double-quantum-single-quantum spectra of 1 – 3

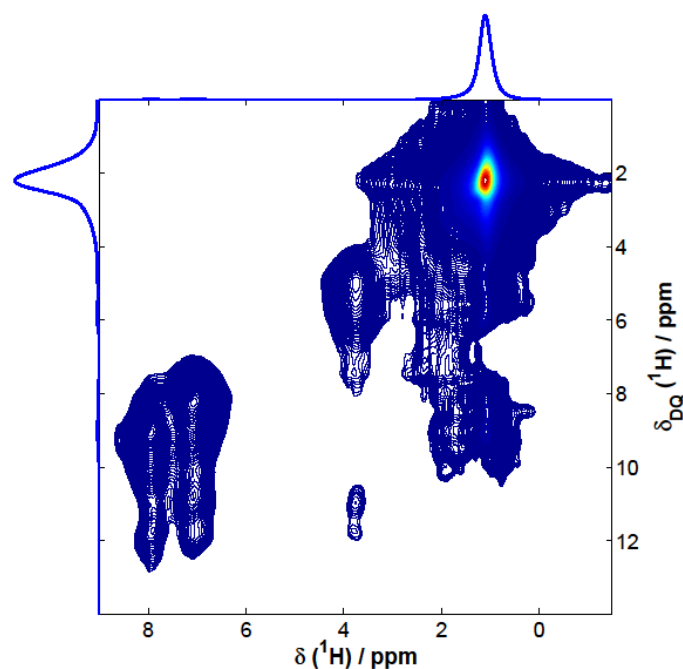


**Fig. S5**  $^1\text{H}$ - $^1\text{H}$  DQ-SQ correlation spectra of compound **1**. The excitation and reconversion time was set to  $80\ \mu\text{s}$  so that only shortest distance correlations are visible. The protons of the  $\text{CH}_3$ -groups are truncated due to the long relaxation times leading to a streak along both the SQ- as well as the DQ-axis in the spectrum.

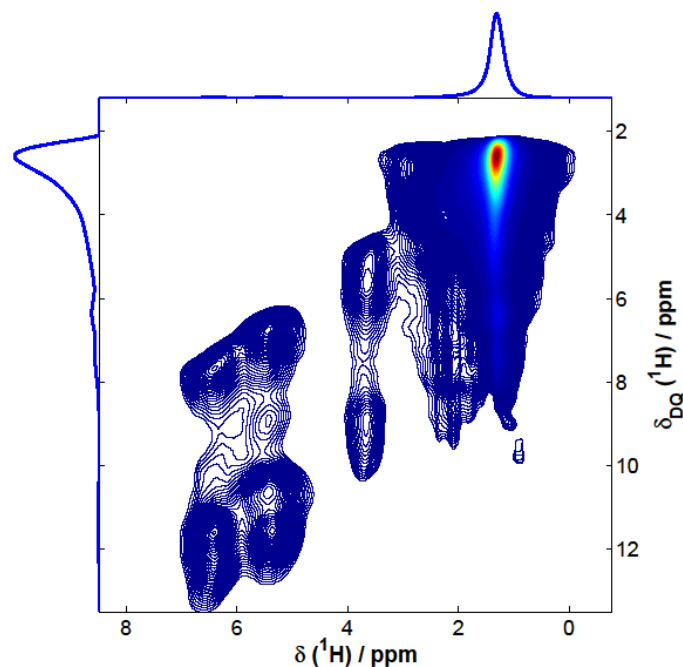


**Fig. S6**  $^1\text{H}$ - $^1\text{H}$  DQ-SQ correlation spectrum of compound **2**. The excitation and reconversion time was set to  $80\ \mu\text{s}$  so that only shortest distance correlations are visible. The protons of the  $\text{CH}_3$ -groups are truncated due to the long relaxation times leading to a streak along both the SQ- as well as the DQ-axis in the spectrum.

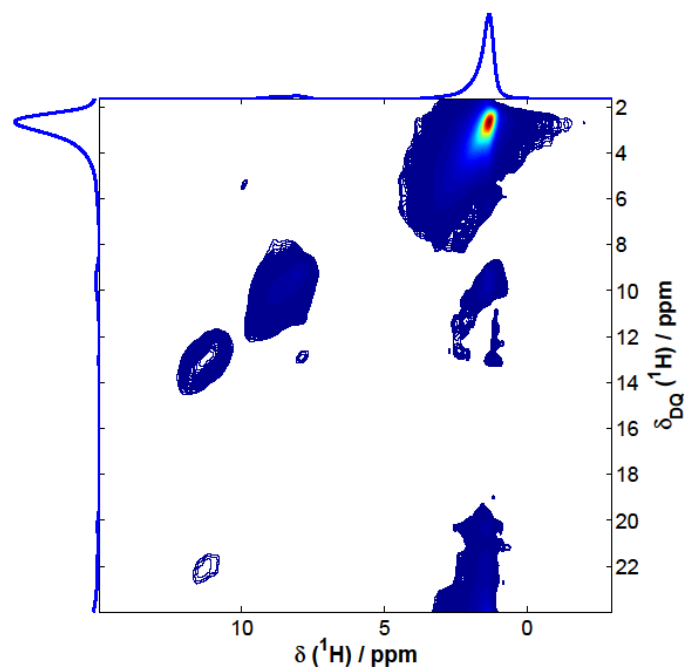


**Fig. S7**  $^1\text{H}$ - $^1\text{H}$  DQ-SQ correlation spectrum of compound **3**. The excitation and reconversion time was set to  $80\ \mu\text{s}$  so that only shortest distance correlations are visible. The protons of the  $\text{CH}_3$ -groups are truncated due to the long relaxation times leading to a streak along both the SQ- as well as the DQ-axis in the spectrum.

### Rietveld profile plots of 2 and 3

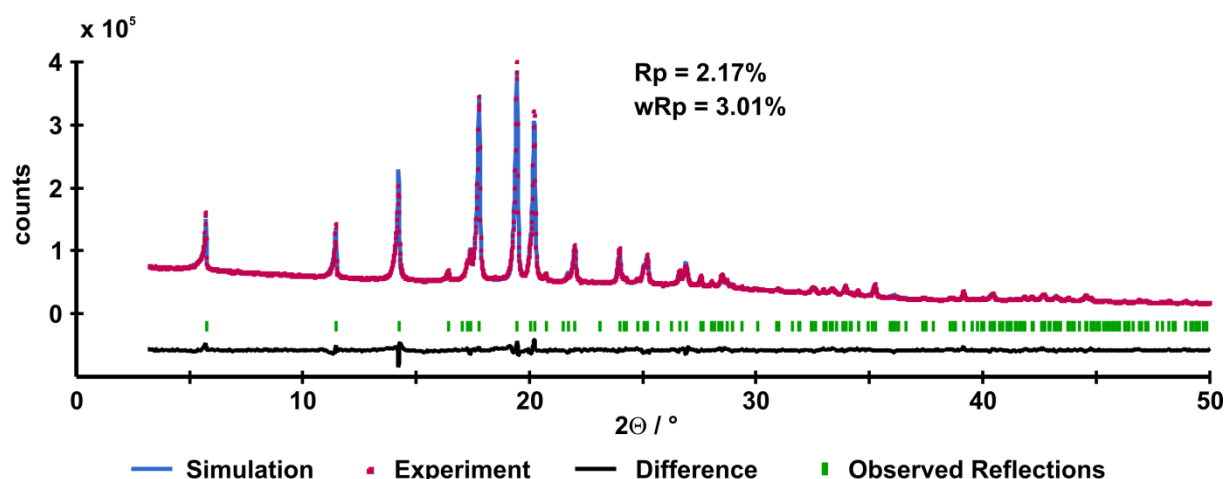


**Fig. S8** Rietveld profile plot of compound **2** measured at room temperature in the  $2\theta$  range of  $3^\circ - 50^\circ$  using  $\text{CuK}\alpha_1$  radiation ( $\lambda = 1.5406 \text{ \AA}$ ).

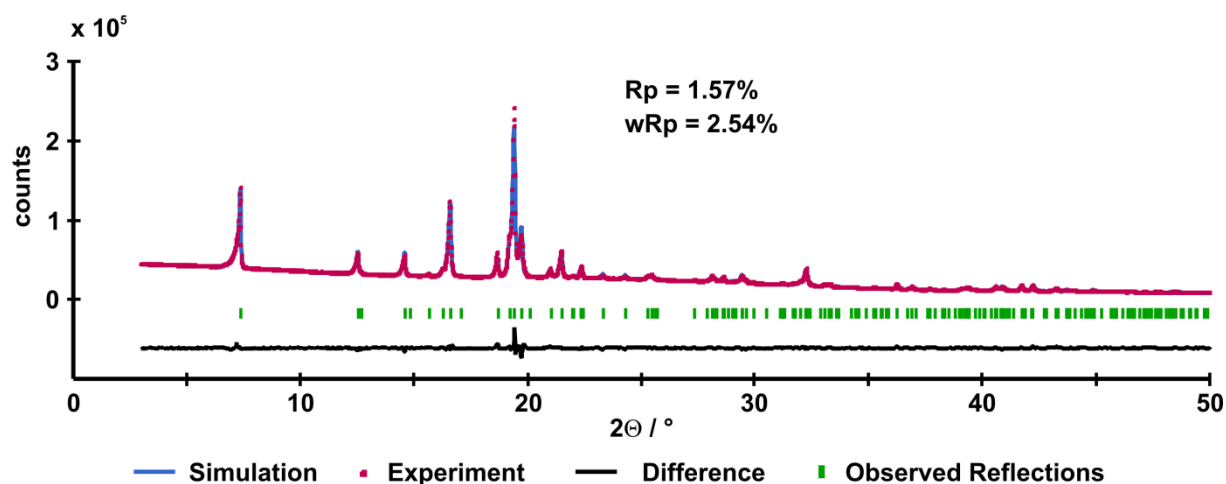


**Fig. S9** Rietveld profile plot of compound **3** measured at room temperature in the  $2\theta$  range of  $3^\circ - 50^\circ$  using  $\text{CuK}\alpha_1$  radiation ( $\lambda = 1.5406 \text{ \AA}$ ).

### References

- 1 K. Eichele, *WSolids1 version 1.20.17*, Universität Tübingen, 2012.
- 2 K. Eichele, M. D. Lumsden and R. E. Wasylshen, *J. Phys. Chem.*, 1993, **97**, 8909.
- 3 M. Hesse, H. Meier and B. Zeeh, *Spektroskopische Methoden in der organischen Chemie*, 5th edn., 1995.
- 4 *Predicted NMR data calculated using Advanced Chemistry Development, Inc. (ACD/Labs) Software V12.5* (© 1994-2013 ACD/Labs).